Anacoustic FWI: Implementation and challenges

Scott Keating and Kris Innanen

ABSTRACT

Full-waveform inversion (FWI) estimates subsurface properties by minimizing differences between synthetic and observed data. It is important for the success of FWI that the synthetic modeling can reproduce the physical mechanisms which give rise to the observed data. Attenuation plays a prominent role in wave propagation, and thus its inclusion in FWI is desirable. An anacoustic FWI is not a trivial extension of FWI however, and problems arise when incautiously applying the same optimization, regularization, and frequency band updating strategies. Specific problems like these and some of their solutions are outlined in this report.

INTRODUCTION

Full waveform inversion (FWI) is a technique which attempts to recover the true subsurface parameters by iteratively minimizing the difference between measured data and modeled data generated from the current estimated subsurface parameters (Tarantola (1984), Lailly (1983)). While multiparameter versions of FWI have been formulated and studied, the majority of research on FWI is focused on a single parameter problem, specifically that in which acoustic wave propagation is assumed and density is treated as constant. In this problem, only p-wave velocity varies in the model. This formulation of FWI can be unsatisfactory for a number of reasons. The acoustic physics assumed are not sufficient to describe seismic wave propagation in the earth, where elastic, anisotropic, and attenuative effects can all play a major role. Consequently, the measured data may not be reproducible with an acoustic model, and there is no guarantee that the acoustic model which most closely matches the measured data will be the one which most accurately recovers the true velocity structure of the subsurface. Given that FWI is designed to minimize the misfit between the measured and modeled data, this is a serious concern. Additionally, p-wave velocity may not be the only parameter of interest for a geophysical problem. AVO, AVAZ, and the spectral ratio and frequency shift methods are existing geophysical techniques for the recovery of elastic, anisotropic and attenuation parameters, respectively, and are often useful to geophysicists. If FWI were able to perform the role of one or all of these techniques, its utility would be greatly enhanced.

Much of the research done on multiparameter FWI has focused on full acoustic FWI, which includes density as well as p-wave velocity, and elastic FWI, which recovers three elastic parameters (Tarantola (1986), Choi et al. (2008)). Anisotropic parameters have also been investigated (Barnes et al. (2008)). This paper is focused on anacoustic FWI, and the unique challenges confronted when attenuation is considered.

Anacoustic FWI has previously been investigated, for example in Hak and Mulder (2011), Hicks and Pratt (2001), Malinowski et al. (2011), Kamei and Pratt (2013) and others. In much of this research, however, recovering attenuation is treated as a small change to the classic FWI problem, with little focus on fundamental issues. For example, many authors, when considering attenuation, neglect to include dispersion (which is physically

necessary). Hak and Mulder (2011) demonstrated that dispersion is necessary to resolve between otherwise ambiguous velocity and attenuation models. This report is not focused on an immediately practical implementation of anacoustic FWI, but rather on hazards like this and the means of navigating them which will be necessary in a practical anacoustic FWI.

THEORY

Anacoustic FWI

Full waveform inversion performs a numerical optimization to minimize a misfit function, which quantifies the discrepancy between measured seismic data, and the data predicted by numerical modeling on a subsurface model. This optimization is done with respect to the parameters of the subsurface model. The most commonly used misfit function in FWI is given by

$$\phi(\mathbf{m}) = \frac{1}{2}||\mathbf{d}_{obs} - \mathbf{d}_{mod}||_2^2 \quad, \tag{1}$$

where ϕ, the misfit, is a function of the subsurface model $\mathbf{m}$ which measures the discrepancy between the measured data $\mathbf{d}_{obs}$ and the modeled data $\mathbf{d}_{mod}$. There are many methods by which this misfit function can be minimized. One of the most effective, albeit costly methods is to iteratively apply the Newton update, given by

$$\mathbf{u} = -\mathbf{H}^{-1}\mathbf{g} \quad, \tag{2}$$

where the gradient, $\mathbf{g}$, is given by

$$\mathbf{g} = \nabla_{\mathbf{m}}\phi = \Re\{\mathbf{J}^t(\mathbf{d}_{obs} - \mathbf{d}_{mod})\} = \Re\{\mathbf{J}^t\delta\mathbf{d}\} \quad, \tag{3}$$

the Hessian, $\mathbf{H}$, is given by

$$\mathbf{H} = \nabla_{\mathbf{m}}^2\phi = \Re(\mathbf{J}^t\mathbf{J}^*) + \Re\left\{\left(\frac{\partial\mathbf{J}}{\partial\mathbf{m}}\right)(\delta\mathbf{d}^*...\delta\mathbf{d}^*)\right\} \quad, \tag{4}$$

and the Jacobian, $\mathbf{J}$, by

$$\mathbf{J} = \frac{\partial\mathbf{d}_{mod}}{\partial\mathbf{m}} \quad. \tag{5}$$

While the Newton update is a very effective update direction, it is typically much too expensive to calculate in FWI, as $\mathbf{H}$ is usually exceedingly large, and thus impractical to store and invert. Most formulations of FWI instead use some approximation to the full Newton update. These approximations include the Gauss Newton update, the truncated Newton update, quasi-Newton methods, the conjugate gradient method and the steepest descent method.

In this paper, the Gauss Newton update is used. This update is obtained by calculating the Newton update as in equation 2, with $\mathbf{H}$ replaced with $\mathbf{H}_{GN}$, where

$$\mathbf{H}_{GN} = \Re(\mathbf{J}^t\mathbf{J}^*) \quad. \tag{6}$$

The Gauss Newton Hessian neglects the residual dependent part of the full Newton Hessian, and is consequently less expensive to compute. The problems associated with inverting a large Hessian matrix persist however. As a result, the synthetic models tested in this report are very small to allow for the computations to be tractable.

Forward Modeling

The frequency domain modeling approach was adopted in this research for several reasons. Firstly, it is usually necessary to employ a multiscale approach in FWI (Bunks et al. (1995)), where early iterations consider only low frequency information and high frequency information is gradually introduced at later iterations. The frequency domain lends itself to this approach, as it allows for efficient methods which only model the frequencies that are used at each iteration. Secondly, constant Q attenuation of the form studied here is difficult to model in the time domain, requiring the use of convolutional operators, whereas in the frequency domain it is relatively simple to introduce these attenuation terms. The anacoustic wave propagation we consider in this report is given by

$$\left[\omega^2 s(\mathbf{r}) + \nabla^2 \right] u(\mathbf{r}, \omega) = f(\mathbf{r}, \omega) \quad , \tag{7}$$

where the model parameter s is given by

$$s(\mathbf{r}, \omega) = \frac{1}{c^2(\mathbf{r})} \left\{ 1 + \frac{1}{Q(\mathbf{r})} \left[i - \frac{2}{\pi} \log \left(\frac{\omega}{\omega_0} \right) \right] \right\} \quad , \tag{8}$$

c is the acoustic wave velocity, Q is the quality factor, ω_0 is a reference frequency, u is the pressure field, and f is a source term. This equation is solved for u by the frequency domain finite difference (FDFD) method. In FDFD, the x second derivative operators are discretized as

$$\frac{\partial^2 \mathbf{u}}{\partial x^2} = \frac{u_{h-1,j} - 2u_{h,j} + u_{h+1,j}}{\Delta x^2} \quad , \tag{9}$$

where Δx is the x spacing of the model, and $u_{h,j}$ denotes the pressure field at the hth x position and jth z position (Franklin (2005)). The expression for the discretization of the z second derivative operators is similar. With the discretized derivative operators, equation 7 can be restated as

$$\left[\omega^2 s_{h,j} u_{h,j} + \frac{u_{h-1,j} - 2u_{h,j} + u_{h+1,j}}{\Delta x^2} + \frac{u_{h,j-1} - 2u_{h,j} + u_{h,j+1}}{\Delta z^2} \right] = f_{h,j} \quad . \tag{10}$$

If positions are mapped to a single 1D index k via $k = (h - 1) * N + j$, we can follow Franklin (2005) and restate eq. 10 as

$$\mathbf{M}\mathbf{u} = \mathbf{f} \quad , \tag{11}$$

where $\mathbf{u}$ and $\mathbf{f}$ are vectors, and $\mathbf{M}$ is a sparse matrix. Equation 11 can then be solved for $\mathbf{u}$.

Equation 10 is valid for the interior of the model, but cannot be applied on the outer edges, where we require an alternate finite difference scheme. In order to avoid unwanted reflections at the model edge, it is important that we adopt absorbing boundary conditions.

In this research, first order Enquist boundary conditions were used. While more sophisticated absorbing boundary conditions are available, such as higher order Enquist boundary conditions and perfectly matched layers, boundary reflections were found to have limited impact on the results in this research. The first order Enquist boundary conditions are designed to produce no reflection for a normal incidence plane wave. They are given by

$$\frac{\partial \mathbf{u}}{\partial n} - i\frac{\omega}{c} = 0 \quad , \tag{12}$$

where n is the direction normal to the interface (Clayton and Enquist (1977)). Depending on the edge in question, this can be discretized using the forward or backward finite difference approximation, and is given for example at the top of the model by

$$\frac{u_{h,2} - u_{h,1}}{\Delta z} - i\frac{\omega}{c_{h,1}} = 0 \quad . \tag{13}$$

In this research report, the spatial resolution used was 10m. The models studied were 500m by 500m.

Gradient and Hessian for the anacoustic case

While equations 3, 6 can be used to compute the gradient and Hessian, it is impractical and unnecessary to explicitly calculate the Jacobian. Instead, we follow (Innanen (2015)) and calculate the gradient using

$$g_c(\mathbf{r}) = \sum_{\mathbf{r}_g, \mathbf{r}_s} \int d\omega \omega^2 (1 + \beta(\omega) s_{q_0}(\mathbf{r})) G_0(\mathbf{r}_g, \mathbf{r}) G_0(\mathbf{r}, \mathbf{r}_s) \delta d^*(\mathbf{r}_g, \mathbf{r}_s) \tag{14}$$

and

$$g_q(\mathbf{r}) = \sum_{\mathbf{r}_g, \mathbf{r}_s} \int d\omega \omega^2 \beta(\omega) s_{c_0}(\mathbf{r}) G_0(\mathbf{r}_g, \mathbf{r}) G_0(\mathbf{r}, \mathbf{r}_s) \delta d^*(\mathbf{r}_g, \mathbf{r}_s) \quad , \tag{15}$$

where $s_{c_0} = \frac{1}{c^2}$, $s_{q_0} = \frac{1}{Q}$, $G_0(\mathbf{r}, \mathbf{r}_s)$ is the Green's function in the recovered medium with a source at $\mathbf{r}_s$, and

$$\beta = i - \frac{2}{\pi} \log\left(\frac{\omega}{\omega_0}\right) \quad . \tag{16}$$

Similarly, the Gauss Newton Hessian can be calculated using

$$H_{cc}(\mathbf{r}, \mathbf{r}') = \sum_{\mathbf{r}_g, \mathbf{r}_s} \int d\omega \omega^4 (1 + \beta(\omega) s_{q_0}(\mathbf{r}'))(1 + \beta(\omega) s_{q_0}(\mathbf{r})) G_0^*(\mathbf{r}_g, \mathbf{r}') G_0^*(\mathbf{r}', \mathbf{r}_s) G_0(\mathbf{r}_g, \mathbf{r}) G_0(\mathbf{r}, \mathbf{r}_s) \quad , \tag{17}$$

$$H_{cq}(\mathbf{r}, \mathbf{r}') = \sum_{\mathbf{r}_g, \mathbf{r}_s} \int d\omega \omega^4 \beta(\omega) s_{c_0}(\mathbf{r}'))(1 + \beta(\omega) s_{q_0}(\mathbf{r})) G_0^*(\mathbf{r}_g, \mathbf{r}') G_0^*(\mathbf{r}', \mathbf{r}_s) G_0(\mathbf{r}_g, \mathbf{r}) G_0(\mathbf{r}, \mathbf{r}_s) \quad , \tag{18}$$

$$H_{qc}(\mathbf{r}, \mathbf{r}') = \sum_{\mathbf{r}_g, \mathbf{r}_s} \int d\omega \omega^4 (1 + \beta(\omega) s_{q_0}(\mathbf{r}')) \beta(\omega) s_{c_0}(\mathbf{r}) G_0^*(\mathbf{r}_g, \mathbf{r}') G_0^*(\mathbf{r}', \mathbf{r}_s) G_0(\mathbf{r}_g, \mathbf{r}) G_0(\mathbf{r}, \mathbf{r}_s) \quad , \tag{19}$$

and

$$H_{qq}(\mathbf{r},\mathbf{r}') = \sum_{\mathbf{r}_g,\mathbf{r}_s} \int d\omega \omega^4 \beta(\omega) s_{c_0}(\mathbf{r}')) \beta(\omega) s_{c_0}(\mathbf{r}))) G_0^*(\mathbf{r}_g,\mathbf{r}') G_0^*(\mathbf{r}',\mathbf{r}_s) G_0(\mathbf{r}_g,\mathbf{r}) G_0(\mathbf{r},\mathbf{r}_s) \quad .$$

(20)

These can then be used to calculate a Gauss Newton update by solving

$$\left[\begin{array}{cc} \mathbf{H}_{cc} & \mathbf{H}_{cq} \\ \mathbf{H}_{qc} & \mathbf{H}_{qq} \end{array} \right] \left[\begin{array}{c} \mathbf{u}_c \\ \mathbf{u}_q \end{array} \right] = \left[\begin{array}{c} \mathbf{g}_c \\ \mathbf{g}_q \end{array} \right]$$

(21)

for velocity and Q model updates $\mathbf{u}_c$ and $\mathbf{u}_q$.

OBSTACLES

There are a number of obstacles which arise in multiparameter anacoustic FWI which are not present in the monoparameter acoustic case. Among these challenges are conflicts in determining an appropriate frequency updating scheme, an increase in the importance of the Hessian in the inversion, and an increase in the consequences of applying a regularization scheme. Each of these issues is outlined in greater detail in the following subsections.

Frequency band updating strategies

In FWI, local minima caused by cycle skipping can cause be significantly harmful to results. Consequently, Bunks et al. (1995) have suggested employing a multiscale approach to FWI. The motivation behind this approach is to avoid local minima caused by high frequency information in the objective function by first minimizing the objective function where only the lowest frequency information is considered, and then slowly introducing higher frequencies on following iterations. Ideally, as higher frequencies are introduced, the associated local minima are avoided because the previous estimates are already in the region of the global minimum. This approach is widespread in FWI as it is currently used.

Multiparameter anacoustic FWI introduces an additional requirement on the frequency updating scheme. Attenuation is a frequency dependent effect, and so comparing data behaviour at different frequencies is essential for its recovery. This is evident in non FWI approaches for recovering Q, such as the spectral ratio and frequency shift methods, which use changes in the amplitude spectrum to recover an estimate of attenuation (Quan and Harris (1997)). This reliance on frequency dependent effects for the recovery of Q leads to an expectation that we will require a range of frequencies at any given update to accurately recover Q. If we use a small frequency band or single frequencies at each step ofo the inversion, it is likely to introduce cross talk, where data residuals caused by one variable are attributed to another.

Hessian in multiparameter FWI

The Hessian matrix plays a major role in multiparameter FWI. It is largely through the Hessian that crosstalk is mitigated by reducing the attribution of data residuals to the wrong parameters (Innanen (2014), Operto et al. (2013)). Consequently, gradient based methods such as the steepest descent method and the conjugate gradient method which neglect the

Hessian become much less appealing in anacoustic FWI. Methods which more appropriately consider the Hessian, such as quasi-Newton, truncated-Newton, Gauss Newton and Full Newton methods are likely to provide much better results in this case.

Regularization

Full waveform inversion is an ill posed problem, and regularization is required to stabilize the problem. This ill-posed nature manifests itself in a Gauss Newton update through the structure of the Hessian, which is not generally a full rank matrix. Consequently, the inverse Hessian is unstable and non-unique. We can stabilize this problem by adding a regularization term to the objective function. By introducing a regularization term, we better restrict the range of acceptable models, which leads to a stable, full rank Hessian matrix. Unfortunately, introducing this term results in a solution which does not exactly solve the original problem. In many applications, this effect has a minimal impact on the quality of the solution to the regularized problem. In multiparameter anacoustic FWI, however, there are interesting effects which arise when regularization terms are introduced, notably affecting cross-talk.

The regularization scheme which was used in this research is designed to minimize the spatial gradient of the update at each iteration. We introduce this regularization by redefining the objective function as

$$\Phi(\mathbf{m}) = \phi(\mathbf{m}) + R(\mathbf{m}) \quad, \tag{22}$$

where

$$R(\mathbf{m}) = ||\nabla(\mathbf{m} - \mathbf{m}_0)||^2 \quad, \tag{23}$$

$\mathbf{m}_0$ is the recovered model at the previous iteration, and ∇ here is the first order central finite difference operator for the spatial gradient, a sparse matrix. This regularization function penalizes model updates with rapid spatial variations in an attempt to stabilize the inversion, but applies no explicit penalties to any particular final inversion result. The contribution to the gradient term by this regularization function is given by

$$\frac{\partial R}{\partial \mathbf{m}} = \left\{ \nabla^T[\nabla(\mathbf{m} - \mathbf{m}_0)] + \left[\nabla^T[\nabla(\mathbf{m} - \mathbf{m}_0)]\right]^T \right\} \quad. \tag{24}$$

In an FWI update, the gradient will be evaluated at the recovered model from the previous iteration, so $\mathbf{m} = \mathbf{m}_0$ when evaluating the gradient, and the contribution in eq 24 will always be zero. The contribution to the Hessian matrix by this regularization function is given by

$$\frac{\partial^2 R}{\partial \mathbf{m}^2} = 2\nabla^2 \quad. \tag{25}$$

Other regularizations tested were found to provide similar results in terms of stability and crosstalk for the examples tested.

NUMERICAL EXAMPLES

In order to demonstrate some of the challenges described in the previous section, some tests on a simple model were conducted. This model is shown in figure (1). The initial
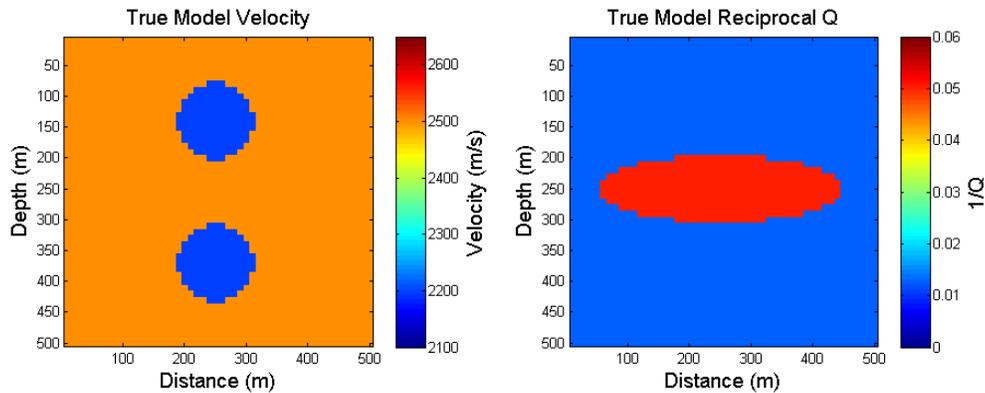
FIG. 1. True model. Left: Velocity. Right: Reciprocal Q. The background velocity is 2500 m/s, anomalies are 2200 m/s. The background Q value is 80, the anomaly Q is 20.

model for the inversion was simply a homogeneous medium with a velocity of 2500 m/s and a Q value of 80. The 'measured' data was generated using the true model and the same forward modeling as was used in the FWI. In these examples, receivers were placed at lateral positions from 15m to 485m with spacings of 10m, at a depth of 7.5m. The sources were placed at lateral positions from 15m to 475m with spacings of 20m, at a depth of 12.5m. While a wavelet could easily have been included, the data was generated using a uniform amplitude spectrum, to simplify the analysis.

Frequency band updating strategies

In order to demonstrate the effect of frequency band size, several different frequency updating strategies were tested. In each case a Gauss Newton optimization was used, with a regularization factor of 1. Figure 2 shows the result of an anacoustic FWI in which a single frequency is inverted at each iteration in 25 steps from 1 Hz to 25 Hz. It is evident by comparing the recovered velocity and Q models that there is severe cross talk in this case. The relative difficulty of updating either parameter independently has also prevented the Q anomaly from being recovered. This has contributed to the poor recovery of the velocity anomaly that lies below the Q anomaly.

In figure 3, an alternate updating scheme is shown in which at each iteration, 6 frequencies in a 1 Hz band were inverted. This band moved in 1Hz increments from 1Hz-2Hz to 24Hz-25Hz. One iteration was performed at each frequency band. The recovered model in this updating scheme shows a clear improvement over the single frequency approach. Cross-talk is significantly reduced, but artifacts remain evident, especially in the recovered Q model, where recovered features closely match velocity anomalies.

A third updating scheme is applied to obtain the results in figure 4. In this example six frequencies, evenly spaced from 1Hz to a maximum frequency, were inverted. This maximum frequency was increased from 2Hz to 25Hz in 1Hz increments. One iteration was performed at each frequency band. Figure 4 demonstrates that this broader frequency band leads to even better results, and a further reduction in cross-talk.
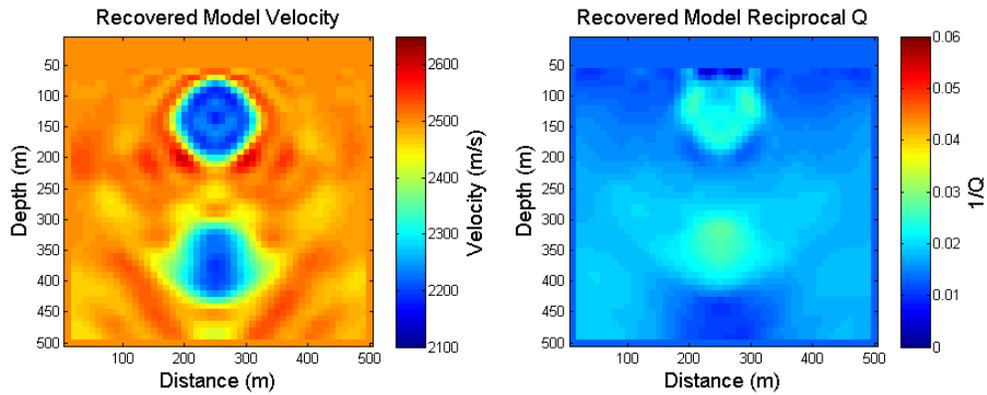
FIG. 2. Result of Gauss Newton FWI using only one frequency at each iteration. Left: Recovered velocity. Right: Recovered reciprocal Q. Considerable cross-talk is readily apparent, contributing to the very poor reconstruction of the attenuation model.
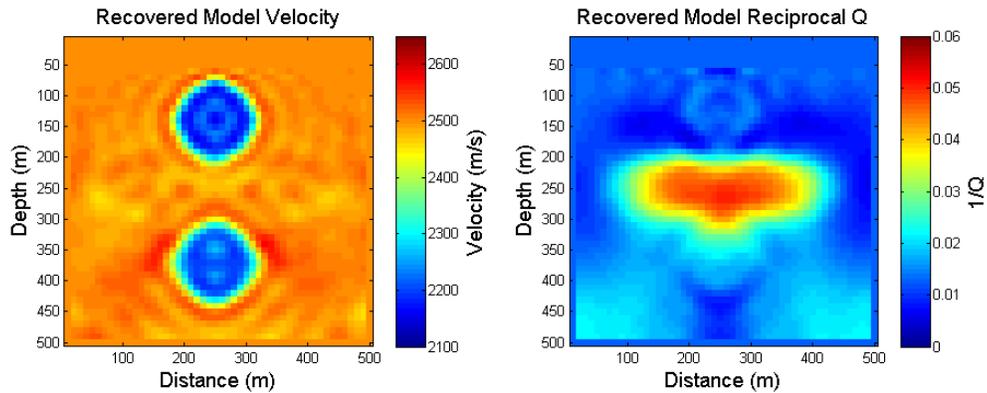
FIG. 3. Result of Gauss Newton FWI using a small frequency band at each iteration. Left: Recovered velocity. Right: Recovered reciprocal Q. Considerable improvement is evident as compared to figure 2, but evidence of cross talk is still apparent, especially in the recovered attenuation.
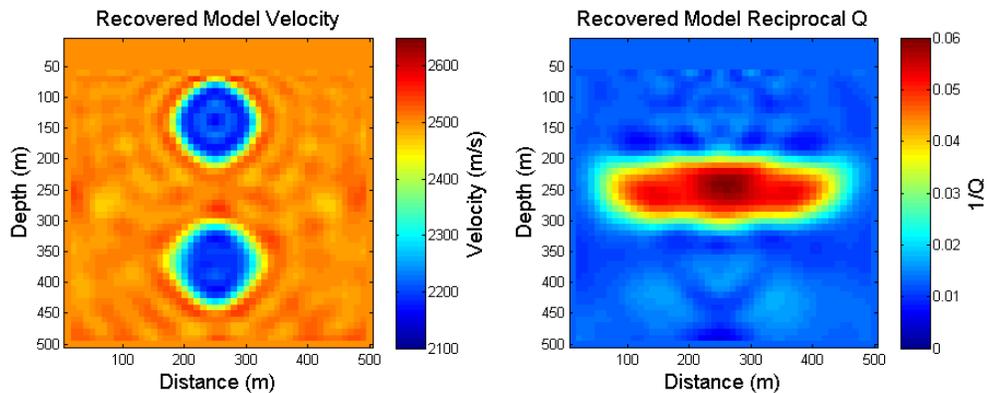
FIG. 4. Result of Gauss Newton FWI using a broad frequency band at each iteration, regularization factor of 1. Left: Recovered velocity. Right: Recovered reciprocal Q. Some cross talk persists, but there is noticeable improvement over figure 3
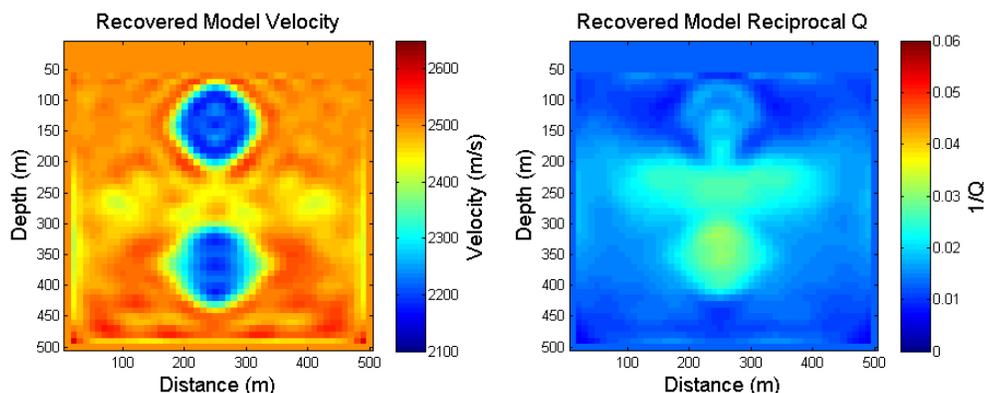
FIG. 5. Result of conjugate gradient FWI using a broad frequency band at each iteration, regularization factor of 1. Left: Recovered velocity. Right: Recovered reciprocal Q. Extreme crosstalk is present, the features of the recovered models are very similar and both recover significant amplitudes at locations where anomalies in the other parameter are present.

Optimization

As discussed above, the Hessian plays a major role in cross-talk suppression in multiparameter FWI. In order to highlight this importance, a conjugate gradient based FWI was tested to compare with the Gauss Newton result shown in figure 4. The same regularization factor and frequency bands were used as for figure 4, but 20 iterations were performed at each frequency band to help compensate for the slower convergence rate of the conjugate gradient method. This value was chosen based on tests which indicated that in the acoustic case results comparable to the GN result could be obtained with this number of CG iterations. The results of this example are shown in figure 5. As anticipated, the neglect of the Hessian matrix has coincided with considerable crosstalk.

Regularization and Stability

To demonstrate the effects of regularization, several regularization factors were tested. Figure 4 shows the result using a regularization factor of 1. Figure 6 shows the result when the regularization factor used is 10^3. As discussed previously, figure 4 is a result close to the answer we would hope to have. Figure 6 by contrast shows significant crosstalk artifacts, and does a poor job of reconstructing the true model. The shift in the solution introduced by regularization is clearly having undesirable effects in the large regularization factor case. This demonstrates the necessity of using as small a regularization term as possible, in order to avoid cross-talk problems.

Figures 4 and 6 show results in a noise-free case. In reality however, unwanted noise is an inevitability in seismic data. As noise increases, the demands on the stability of our inversion also increase. Figures 7 and 8 show the results of inversions using the same parameters as figures 4 and 6, but with noise introduced. The noise used was normally distributed random noise, with a signal to noise ratio of 10, where signal is taken to be the measured data with the direct arrivals removed. The effects of noise are pronounced in figure 7, where a smaller regularization factor is used, and are significantly detrimental to the recovered result. In comparison, the effects of noise in figure 8 are exceedingly minor,
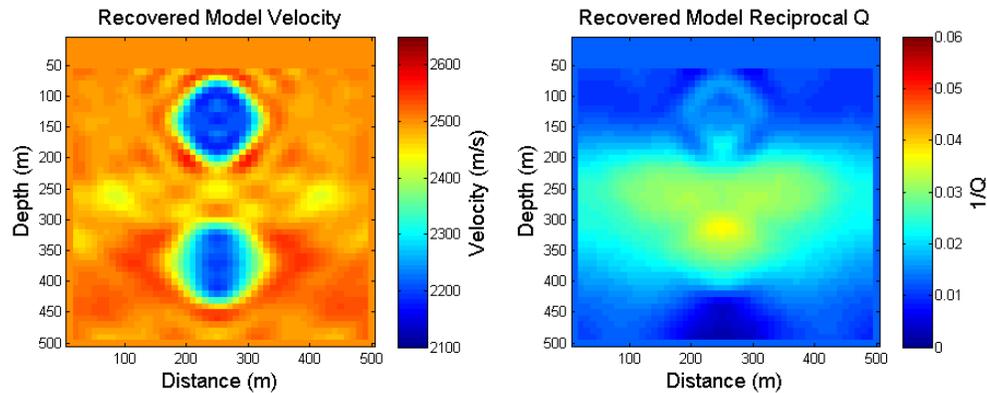
FIG. 6. Result of Gauss Newton FWI using a regularization factor of 1000. Left: Recovered velocity. Right: Recovered reciprocal Q. In comparison with the small regularization factor case (figure 4) there is considerable crosstalk, and attenuation is poorly reconstructed.
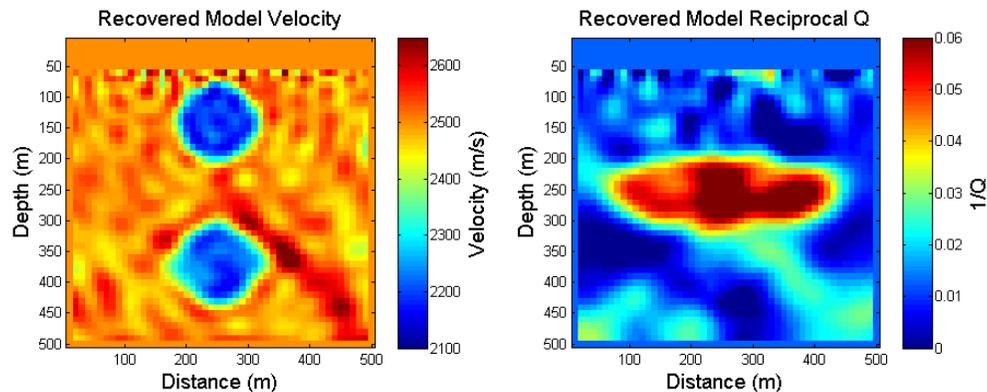
FIG. 7. Result of Gauss Newton FWI using a regularization factor of 1, signal to noise ratio of 10. Left: Recovered velocity. Right: Recovered reciprocal Q. High amplitude, unpredictable changes from the noise free case (figure 4) are clear. Regularization here is too small to recover a reliable result.

due to the much larger regularization factor. An intermediate regularization factor may be expected to outperform these examples. Figure 9 shows the equivalent result with noisy data and regularization factor of 10. In this example, this value seems to provide a good compromise between inaccuracies caused by regularization and those caused by noise.

All regularizations investigated in this research displayed the same trade-off between stability and cross-talk, but differed in the extent of this trade-off. Determining a regularization scheme which maximizes the stability at a given level of crosstalk is a subject of ongoing investigation. Alternate approaches where stability is achieved by iteratively solving a system with a shrinking regularization factor are also being studied.

CONCLUSIONS

There are several factors which complicate multiparameter anacoustic FWI as compared to monoparameter acoustic FWI. Gradient based methods which entirely neglect the Hessian become impractical due to crosstalk between parameters. Frequency updating schemes are confronted with the need to provide sufficient information to distinguish be-
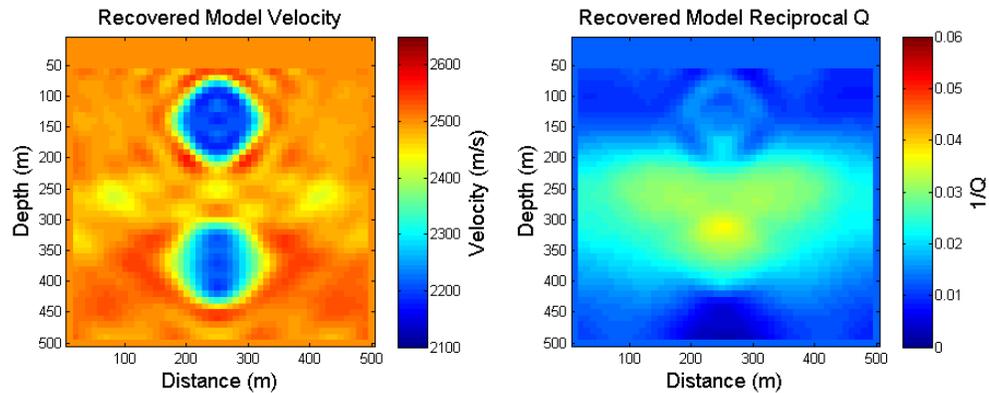
FIG. 8. Result of Gauss Newton FWI using a regularization factor of 1000, signal to noise ratio of 10. Left: Recovered velocity. Right: Recovered reciprocal Q. Changes from the noise free case (figure 6) are negligible. The large regularization has contributed significant robustness to noise.
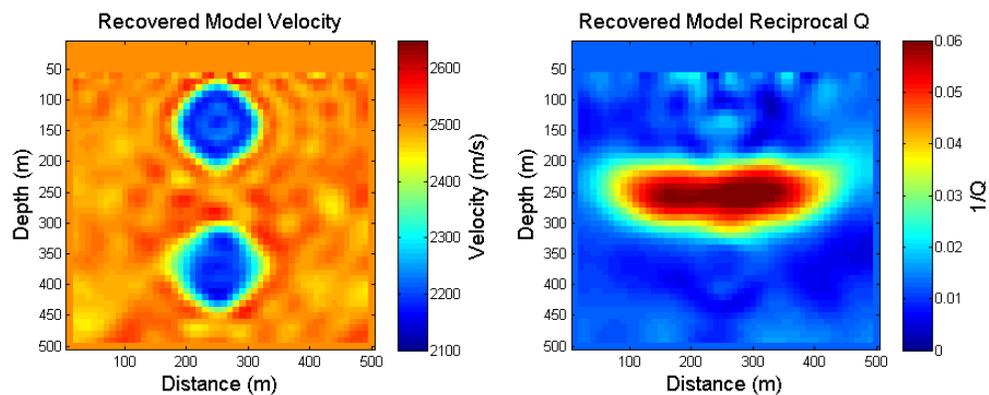
FIG. 9. Result of Gauss Newton FWI using a regularization factor of 10, signal to noise ratio of 10. Left: Recovered velocity. Right: Recovered reciprocal Q. Significant improvements from figures 7 and 8 are noticeable when using this intermediate regularization factor.

tween velocity and attenuation effects while still preserving the multiscale approach. Regularizations are necessary to provide stability to the system, but tend to introduce cross-talk in doing so. A successful implementation of anacoustic full waveform inversion will likely need to address each of these issues.

ACKNOWLEDGMENTS

REFERENCES

Barnes, C., Charara, M., and Tsuchiya, T., 2008, Feasibility study for an anisotropic full waveform inversion of cross-well data: Geophysical Prospecting, **56**.

Bunks, C., Salek, F., Zaleski, S., and Chavent, G., 1995, Multiscale seismic waveform inversion: Geophysics, **60**.

Choi, Y., Min, D., and Shin, C., 2008, Two-dimensional waveform inversion ofmulti-component data in acoustic-elastic coupled media: Geophysical Prospecting, **56**.

Clayton, R., and Enquist, B., 1977, Absorbing boundary conditions for acoustic and elastic wave equations: Bulletin of the Seismological Society of America, **67**.

Franklin, J., 2005, Frequency domain modeling techniques for the scalar wave equation, an introduction: MIT Earth Resources Laboratory Industry Consortia Annual Report, 1–22.

Hak, B., and Mulder, W., 2011, Seismic attenuation imaging with causality: Geophysical Journal International, **184**.

Hicks, G., and Pratt, R., 2001, Reflection waveform inversion using local descent methods: Estimating attenuation and velocity over a gas-sand deposit: Geophysics, **66**.

Innanen, K., 2014, Seismic avo and the inverse hessian in precritical reflection full waveform inversion: Geophys. J. Int., **199**.

Innanen, K., 2015, Absorption in fwi âĂŞ some questions and answers: CREWES Annual Report, **27**.

Kamei, R., and Pratt, R., 2013, Inversion strategies for visco-acoustic waveform inversion: Geophysical Journal International, **194**.

Lailly, P., 1983, The seismic inverse problem as a sequence of before stack migrations: Conference on Inverse Scattering, Theory and Application, Society for Industrial and Applied Mathematics, Expanded Abstracts, 206–220.

Malinowski, M., Operto, S., and Ribodetti, A., 2011, High-resolution seismic attenuation imaging from wide-aperture onshore data by visco-acoustic frequency-domain full-waveform inversion: Geophysical Journal International, **186**.

Operto, S., Gholami, Y., Prieux, V., Ribodetti, A., Brossier, R., Metivier, L., and Virieux, J., 2013, A guided tour of multiparameter full-waveform inversion with multicomponent data: From theory to practice: The Leading Edge, 1040–1054.

Quan, Y., and Harris, J., 1997, Seismic attenuation tomography using the frequency shift method: Geophysics, **62**.

Tarantola, A., 1984, Inversion of seismic reflection data in the acoustic approximation: Geophysics, **49**.

Tarantola, A., 1986, A strategy for nonlinear inversion of seismic reflection data: Geophysics, **51**.